



Science Arts & Métiers (SAM)

is an open access repository that collects the work of Arts et Métiers Institute of Technology researchers and makes it freely available over the web where possible.

This is an author-deposited version published in: <https://sam.ensam.eu>
Handle ID: <http://hdl.handle.net/10985/24726>

To cite this version :

Doria Taous ATMANI, Mohammed Said BOUAMERENE, Mohammed GACEB, Corinne NOUVEAU, Hamid AKNOUCHE - Improvement of the tribological behavior of TiN/CrN multilayer coatings by modulation wavelength variation - Tribology International - Vol. 192, p.109226 - 2023

Any correspondence concerning this service should be sent to the repository

Administrator : scienceouverte@ensam.eu



Improvement of the tribological behavior of TiN/CrN multilayer coatings by modulation wavelength variation

Taous Doria Atmani^{a,b,*}, Mohammed-Said Bouamerene^b, Mohammed Gaceb^a,
Corinne Nouveau^c, Hamid Aknouche^b

^a Laboratory of Petroleum Equipment Reliability and Materials, M'hamed Bougara University, Independence Avenue, 35000 Boumerdes, Algeria

^b UR-MPE, M'hamed Bougara University, Independence Avenue, 35000 Boumerdes, Algeria

^c Arts et Metiers Institute of Technology, LABOMAP, HESAM University, F-71250 Cluny, France

A B S T R A C T

Keywords:

Multilayer coating
Layer thickness
Surface roughness
Wear resistance

Hard coatings are widely used in materials engineering as surface coatings to protect mechanical parts subject to friction. For a coating to be functionally successful, it should possess high wear resistance. Experimental work has been performed on TiN/CrN multilayer coatings with various modulated periods, deposited on XC48 steel substrates having two different surface roughnesses using reactive direct current magnetron sputtering. Their Tribological performances were investigated following dry sliding wear tests using a tribometer with ball-on-flat contact configuration. The prevailing wear mechanisms of TiN/CrN coatings are dominated by oxidation of wear debris and counter material transfer. The decreased wear rate was significantly influenced by both the reduction of the period thicknesses and the increase of substrate surface roughness. Nonetheless, varying thickness period in the multilayer and increasing the substrate roughness did not show any significant wear resistance improvement.

1. Introduction

Hard thin films are mainly used in mechanical engineering as protective coatings of several types of surfaces. They are better suited for optimizing the wear resistance performance of mechanical parts subjected to aggressive friction stresses, such as machine components [1–3] gas turbine and compressor blades [4–6] as well as machining tools for drilling, cutting and molding [7–9]. In addition, recent improvements in hard thin films properties have made them attractive for biomedical use [10–12]. Besides, the application of transition metal nitrides, as hard thin film to protect coated surfaces, has become a common practice over the last decades [13–15]. Likewise, extensive research conducted on multilayered PVD (physical vapor deposition) coatings obtained by alternatively depositing two chemically and/or mechanically different materials based on nitride transition metal have validated the approach of multilayered architectures for optimizing the performance of coatings. Multilayered coatings have been found to possess improved mechanical and tribological properties, as compared to bulk materials. In

many cases, it has been shown that by layering thin layers of metal nitride (such as VN, NbN, WN, ZrN and CrN) with TiN layers, a high hardness can be obtained [16–19]. These nanostructured multilayer coatings with low period (preferably less than few nm thick) so called superlattices possess properties which can be tailored depending upon the choice, and layer thickness of the constituent materials and deposition parameters. Indeed, the thin films properties depend critically on how they are made. This opens up several opportunities to design new materials with specially tailored desired properties. Among these multilayered coatings which have shown, during the last years, very interesting properties such as high hardness, low coefficient of friction and high temperature stability amongst others, the multilayered coatings made of TiN and CrN nitrides are the most quoted [20–22]. While TiN possesses high hardness, CrN is a tough and superior coating in terms of wear and corrosion resistance. An improvement of material ductility and toughness is important to avoid an uncontrollable fracture. [18] In a prior investigation, the TiN/CrN coating exhibited enhanced hardness by decreasing their period thickness down to 13 nm, the

* Correspondence to: M'Hamed Bougara University - Faculty of Technology - Department of Mechanical Engineering, Independence Avenue, 35000 Boumerdes, Algeria.

E-mail addresses: t.atmani@univ-boumerdes.dz (T.D. Atmani), m.bouamerene@univ-boumerdes.dz (M.-S. Bouamerene), m.gaceb@univ-boumerdes.dz (M. Gaceb), corinne.nouveau@ensam.eu (C. Nouveau), h.agnouche@univ-boumerdes.dz (H. Aknouche).

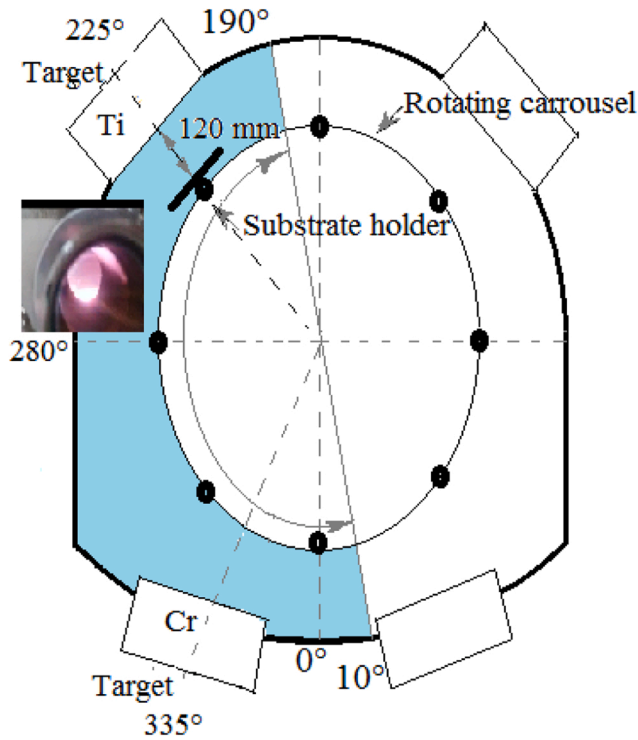


Fig. 1. Schematic illustration of the industrial magnetron sputtering system.

superlattices hardening up to 48.5 ± 1.3 GPa [17]. From these several research, results showed that the presence of a large number of interfaces between individual layers of the multilayer coatings resulted in a considerable increase in hardness, strength and, in some cases, toughness. It is considered that the effect of interface on the mechanical properties is significant when the thickness of the individual layers in the multilayer coatings is at the nanoscale level. Furthermore, coatings that include asymmetrical layer thicknesses exhibit superior hardness properties in comparison to coatings with uniform layer thicknesses. Hence, the precise architectural design of multilayer coatings can then enhance their properties.

The TiN/CrN multilayer coatings find application in various fields, such as automotive components, electronic devices and medical implants. The service behavior of the coated component is mainly determined by the tribological properties of the coating which play a decisive role in determining its performance. However, there are several factors in the tribological behavior which still need to be understood. Increased friction between the contacting bodies not only reduces the mechanical efficiency of the system and increases frictional heating, but also influences the distribution of contact stresses in the near-surface area. Indeed, in dry friction, the interactions and interdependencies between the surfaces are complex as several mechanisms can coexist in the same contact. Interfacial tribological responses of hard coatings are usually characterized by their complexity and variability, as they are influenced by several factors, such as the friction system structure, the operating conditions, and the friction pair materials [23–26]. It is well known that, friction and wear are not intrinsic properties of materials, but only service properties [27]. The service performance of coated components in most engineering applications greatly depends on the coating-substrate bonding strength which is considerably affected by the type of substrate and its surface morphology [15,28–30]. Moreover, the coating tribological performance depends strongly on the surface roughness of the film, it is of great interest to understand and thus control the roughness development during film growth [31,32]. Therefore, evaluating factors that influence friction and wear is of great importance in deepening our understanding of the tribological behavior,

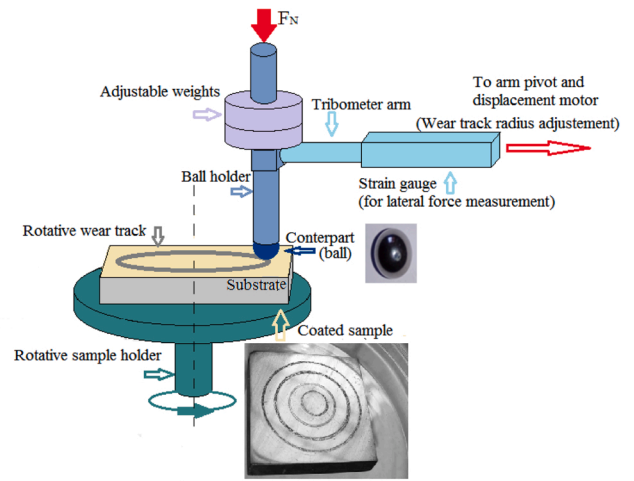


Fig. 2. Scheme of ball-on-flat wear test system.

and ensuring the long-term reliability of mechanical equipment while minimizing energy loss through friction.

In the present paper, the tribological properties of three multilayered TiN/CrN coatings with different layer thicknesses and deposited on substrates with two different surface roughnesses are studied. The substrate surface roughness and the modulation period variation effects on the coefficient of friction and the wear resistance are investigated and then correlated to their structural parameters as well as their mechanical properties previously studied [33]. In addition to the multilayered coatings, corresponding CrN single layer purpose have been included for comparison. All the coatings were deposited using the reactive DC magnetron sputtering process.

2. Experimental details

2.1. Film deposition technique

The samples were prepared by magnetron sputtering in a KENO-SISTEC K540V system having a semi-cylindrical shape (550 mm diameter, 600 mm height and 370 liters). There are four vertically mounted targets (Fig. 1) facing each other on opposite sides of the substrate holder and 120 mm far from the substrate. High purity Ti (99.95%) and Cr (99.99%) materials were used as sputtering targets. The substrate holder can be rotated at 0.25 - 1 rpm to produce nanolayered materials with controlled layer thickness. TiN and CrN bilayers were deposited on single crystal Si (100) ($10 \times 10 \text{ mm}^2$) and two polished (Sa1 and Sa2) XC48 steel substrates groups ($25 \times 25 \times 4 \text{ mm}^3$), by varying the period layer thicknesses for each multilayer. Prior to the coating deposition, the samples were cleaned using the conventional procedure before being mounted in the vacuum chamber. The substrate-holder on which were fixed the steel and Si substrates was moved back and forth between the Cr and Ti targets. In brief, these coatings were grown by direct current magnetron sputtering in vacuum with mixed gas flow of high purity argon (99.999%) and nitrogen (99.999%), at a properly controlled power input, and a suitable substrate bias voltage of -500 V. Detailed experimental procedure: sputtering deposition conditions, microstructure characterizations and mechanical properties, have been reported in our previous paper [33]. During deposition, the substrate temperature was maintained at 300°C . ML1-(Si, Sa1 and Sa2), ML2-(Si, Sa1 and Sa2) and ML3-(Si, Sa1 and Sa2) respective multilayer films with constant sequence $\Lambda = 20$ nm with 1:1 layer ratio, decreasing constant sequence $\Lambda = 12$ nm with 1:1.7 layer ratio and varying sequences $\Lambda = 40$ to 10 nm with 1:1 layer ratio were produced. In addition to the multilayer coatings, homogeneous CrN coatings have been included as reference material. All coatings were close to $2 \mu\text{m}$ thick. The nano-structured

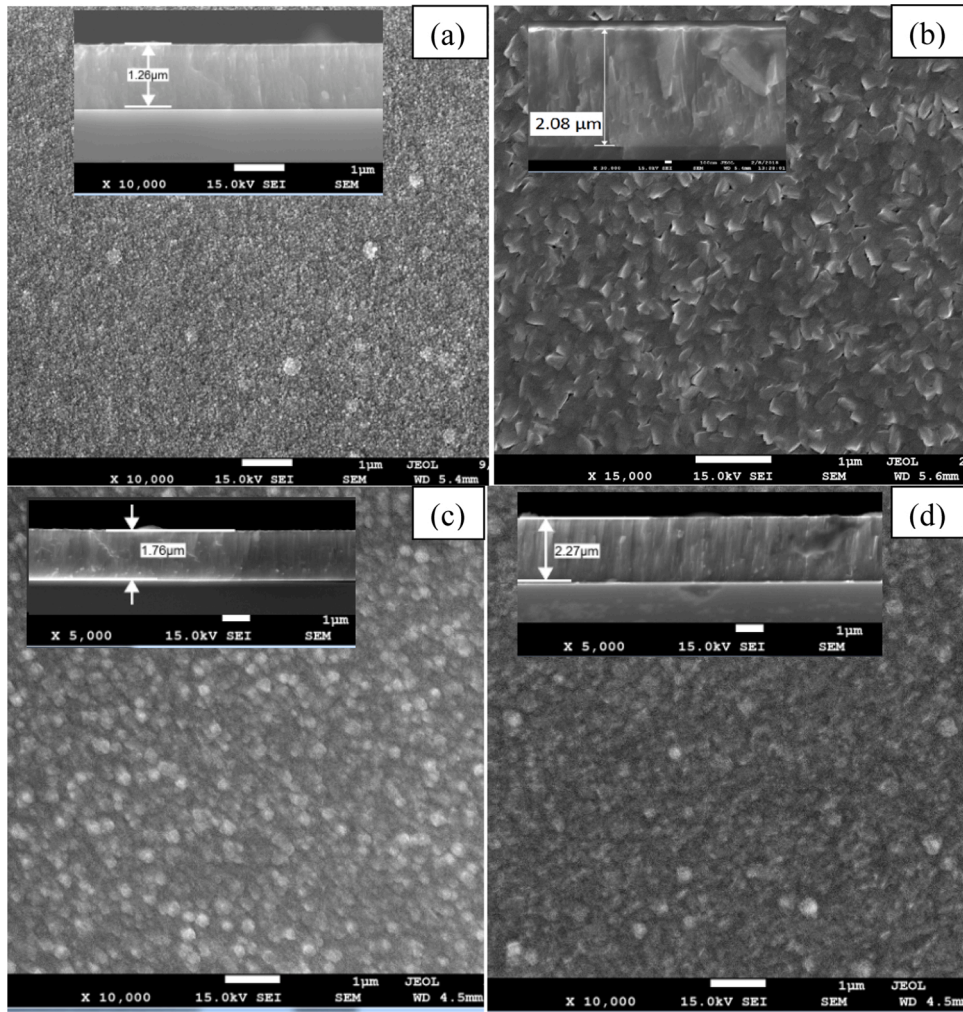


Fig. 3. Top view and cross sectional SEM micrographs of (a) CrN monolayer and TiN/CrN multilayer at (b) $\Lambda = 20$ nm, (c) $\Lambda = 12$ nm and (d) $\Lambda = 40\text{--}10$ nm, deposited on Si substrate.

multilayer coatings obtained showed high hardness from 30 to 43 GPa.

2.2. Characterizations

Friction and wear tests of the films were carried out using a conventional ball-on flat rotative tribometer (TriboX, CSM Instrument), under dry and unlubricated sliding conditions, as illustrated schematically in Fig. 2. The surface of stationary top mounted steel (100Cr6) ball of 6 mm in diameter, used as the counterpart, was rubbed against rotating flat coated samples. The tribometer is equipped with a digital acquisition chain that allows in-situ measurement of test parameter evolutions to be recorded. The usable results are the coefficient of friction (COF) curves corresponding to the materials of the ball-flat pair.

The dry friction tests of all the coated samples were conducted under similar atmospheric conditions, at ambient humidity and laboratory temperature of 24 °C. A normal load of 3 N and a constant sliding speed of 20 cm/s were applied during the friction tests. The friction coefficient was determined after a sliding distance of 50 m. Before each test, the samples and the balls were cleaned and rinsed with acetone in ultrasonic bath. It must be taken into account that the tests were carried out at different times.

The wear track morphologies of as deposited films were examined using Scanning Electron Microscopy (SEM JSM 5900 LV, 15 kV), combined with energy dispersive spectrometry and wavelength dispersive spectrometry (EDS-WDS) Oxford INCA x-act at operating voltages of 15

and 5 kV to allow the TiN/CrN multilayer failure mechanisms and the chemical composition analysis to be assessed overall the worn surface tracks.

Wear track measurement were carried out by a Veeco-Wyko NT 1100 optical profilometer. The scanning procedure generated line profiles of the wear track cross sectional areas. The removed coating volume was then calculated based on this cross sectional areas and the wear track diameter assessed at several locations of the worn surface. The wear rate of the coating was estimated by the Eq(1): $K_v = \frac{V}{L \cdot F_N} H$ where V is the worn volume in mm^3 , L is the sliding distance (m), F_N is the applied normal load (N) and H the hardness of the material tested. The uncoated and coated substrates surface roughness was also measured using the same optical profilometer.

3. Results and discussion

3.1. Coating morphology

Fig. 3 shows the top view and cross-section SEM micrographs of CrN monolayer coating (Fig. 3(a)) and TiN/CrN multilayer coatings deposited at different periods: $\Lambda = 20$ nm ratio 1:1, $\Lambda = 12$ nm ratio 1.7:1, and $\Lambda = 40\text{--}10$ nm ratio 1:1 (Fig. 3(b, c and d), respectively), deposited on Si substrate. The TiN/CrN multilayer coatings exhibited a dense nano-columnar structure. It appears that the stratified structure grain growth is not systematically interrupted by the different interfaces. The

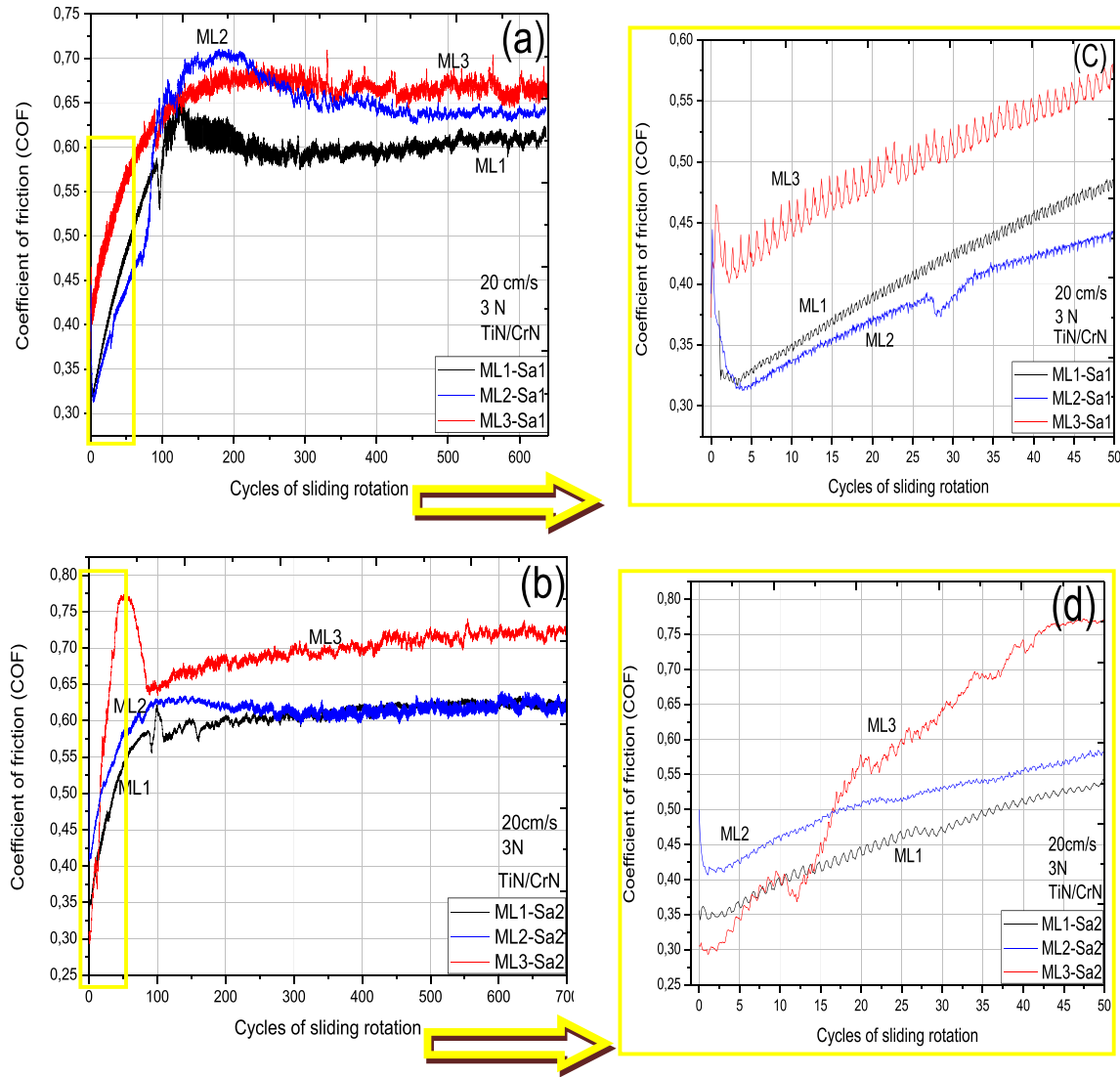


Fig. 4. Coefficient of friction curves of TiN/CrN multilayer coatings deposited at different periods (Λ), as compared with that of XC48 steel substrate, on (a and c) smoother substrate surface Sa1 and (b and d) rougher substrate surface Sa2.

decreased coating period from $\Lambda = 20$ nm to $\Lambda = 12$ nm lead to decrease in the crystallite sizes and surface roughness as opposed to the varying period ($\Lambda = 40$ to 10 nm) coating. The optical scan carried out on the as-deposited CrN-Si, ML1-Si, ML2-Si and ML3-Si specimen surface ($100 \times 100 \mu\text{m}^2$) revealed an average surface roughness of 8.5 nm, 5 nm, 3.5 nm and 7 nm, respectively. The period (Λ) variation affected the crystallite size and very slightly the texture of the films. The residual compressive stress in the coatings promoted the decrease in grain size according to the Hall-Petch relationship. Similar behavior is reported in Refs. [16,17,20,34,35].

3.2. Tribological properties

Fig. 4(a) shows coefficient of friction (COF) curves of TiN/CrN multilayer coatings, deposited at various periods (Λ) on the less rough steel substrates (Sa1), as a function of sliding rotation cycles (rotation number related to the distance traveled), and the inset shows the steel substrate frictional curve. These COF curves exhibited a rapid increase at the beginning of the test, followed by a steady state. Indeed, we can observe at the start of the friction curves, a very short initial period corresponding to the contact under pressure of asperities between the two antagonist surfaces; it is an accommodation phase of ball/coating

materials (lapping). The COF curves of the ML2-Sa1 ($\Lambda = 12$ nm ratio 1.7:1) exhibited the lowest value of about 0.33, followed by the ML1-Sa1 coating ($\Lambda = 20$ nm ratio 1:1) with the COF value of about 0.36. The highest value of about 0.4 was credited to the ML3-Sa1 ($\Lambda = 40$ –10 nm ratio 1:1) as illustrated in Fig. 4(c). These results were in agreement with previous results which showed that there is an increase average surface roughness for the ML2-Sa1, ML1-Sa1 and ML3-Sa1 34 nm, 43 nm and 47 nm coating, respectively [36]. Interactions occurred on the real contact areas which represent only a very small part of the nominal contact surface, resulting in highly concentrated contact stresses [37]. The high concentrated normal and tangential loads were applied on limited number of column grain tops. Consequently, that resulted in an increase of coefficient of friction, which may be gradual (in ML3-Sa1) or abrupt (in ML1-Sa1 and ML2-Sa1). The ML2-Sa1 coating coefficient of friction manifested a rapid increase to reach higher value than that of the ML1-Sa1 coating. Conversely, the ML3-Sa1 coating coefficient of friction manifested a progressive increase to 0.68 along with a small oscillation tendency. Further, its COF curve showed an unstable and fluctuating feature at 300–700 cycles, without any significant decrease. The COF increase is related to wear phase of the nitride coating grains; this period is manifested by disturbance over a certain distance due to fracture, breakage, and spalling wear. The ML1-Sa1 and the ML2-Sa1

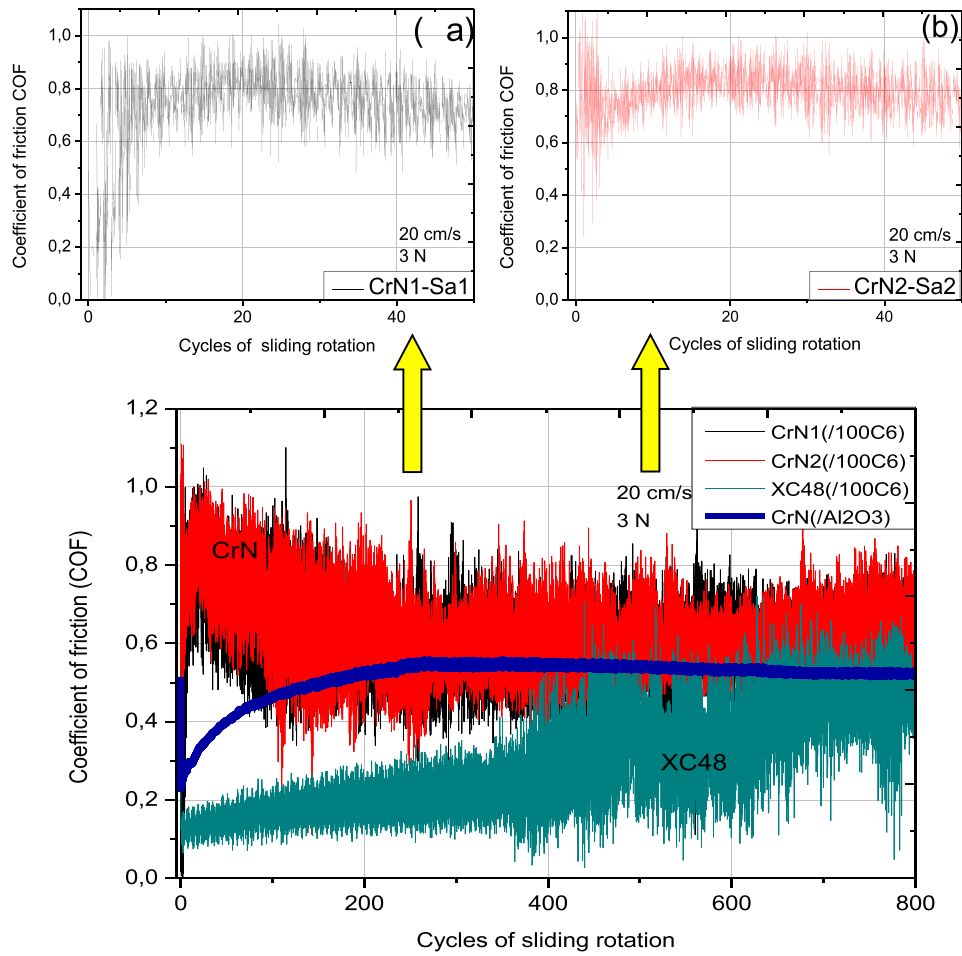


Fig. 5. Coefficient of friction curves of CrN monolayer coatings deposited on XC48 steel substrate with (a) smoother substrate surface Sa1 and (b) rougher substrate surface Sa2.

coatings presented a slow decrease to the steady value of 0.60 and 0.65, respectively. Decrease in friction is related to tribo-layer formation. Indeed, the oxides thus formed TiO_2 and Cr_2O_3 , eventually becoming nano-scale agglomerates that form a bed of individual particles, acting as a solid lubricant, as reported in the literature [38–41]. It's found to change the stress distribution on the wear contact. Beyond that distance traveled, the coefficient of friction tends towards stabilization.

A similar trend in friction was observed on the COF curves of the TiN/CrN multilayer coatings deposited on rougher steel substrates Fig. 4 (b). Similar COF curves evolution was obtained, but the COF values were slightly higher compared to the same coatings deposited on smoother substrates. Besides, as compared to ML1-Sa1 and ML2-Sa1 films

deposited on smoother surface, the ML1-Sa2 film manifested lower value of COF than those of the ML2-Sa2, as shown in the initial dry sliding tests Fig. 4(d). This result doesn't match with the ML2-Sa2, ML1-Sa2 and ML3-Sa2 increased surface roughness (40 nm, 50 nm and 57 nm, respectively).

Concerning the CrN layers, they were also deposited on the Sa1 and Sa2 steel substrate (Fig. 5(a and b, respectively)) and showed approximately the same coefficient of friction variation trend. Its evolution cannot be considered to significantly differ for the two films, except at the beginning of the friction sliding test because of their surface roughness difference ($R_{a1} = 47.5$ nm and $R_{a2} = 56.7$ nm, respectively). Both coefficient of friction values ended up stabilizing at 0.6, higher

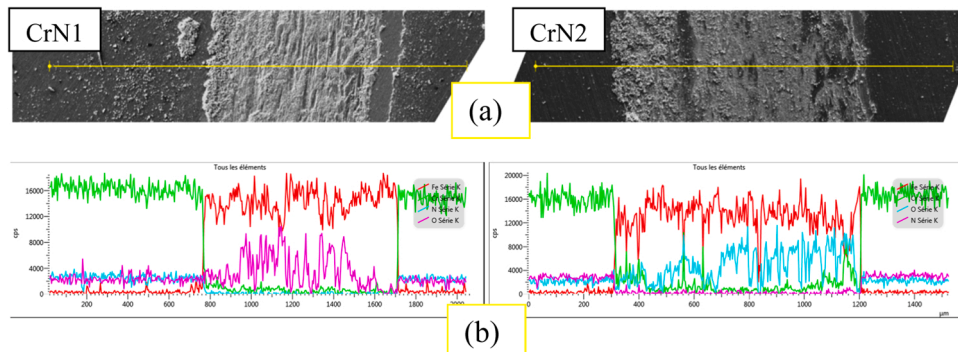


Fig. 6. (a) Worn surface morphologies of CrN-(Sa1 and Sa2) and (b) corresponding EDS profile.

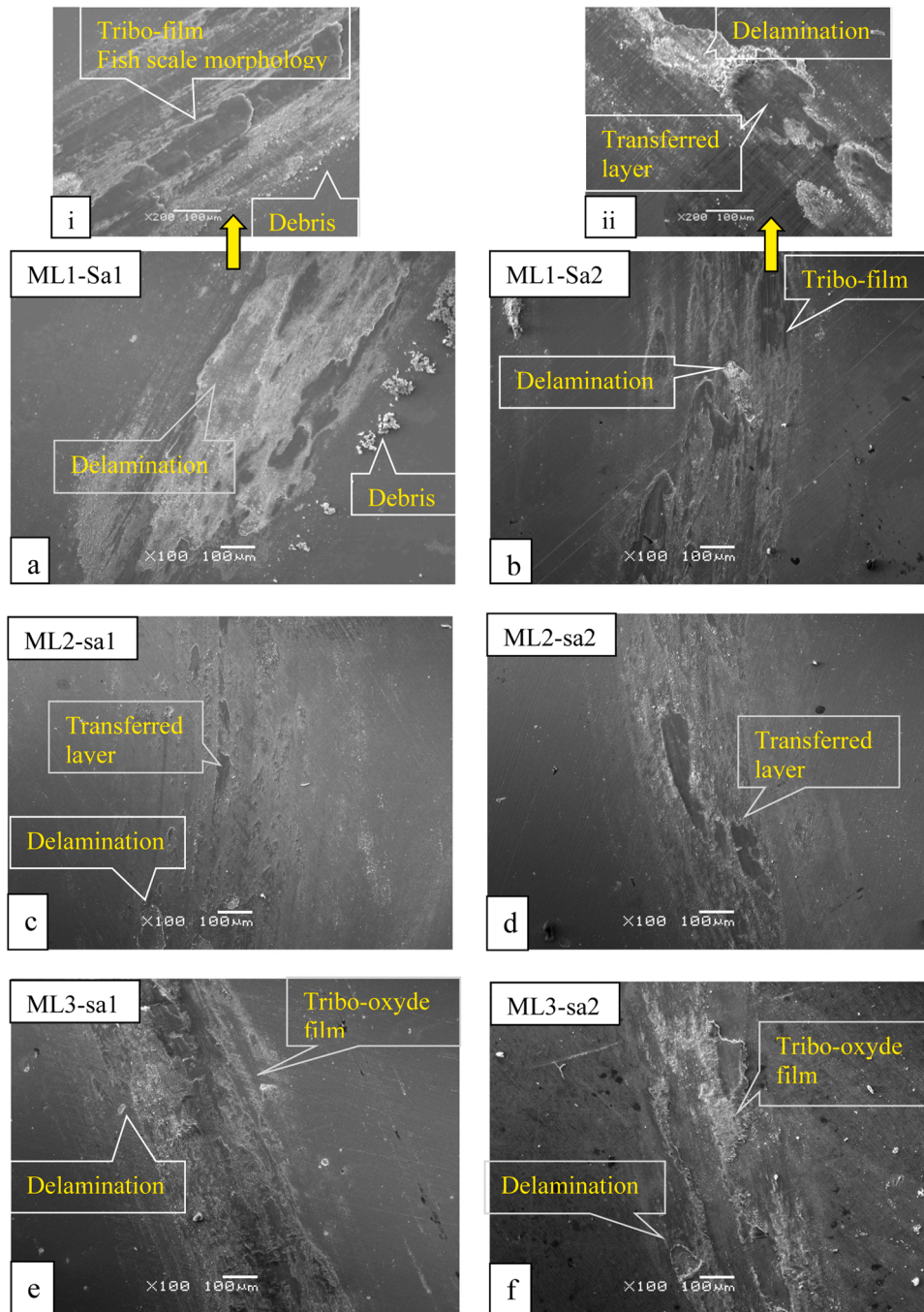


Fig. 7. Worn surface SEM-micrographs of the TiN/CrN multilayered coatings ML1, ML2 and ML3 (with 100 × magnification) deposited on (a, c and e) Sa1 surface substrate and (b, d and f) Sa2 surface substrate. (i and ii) are wear details of ML1 coatings with 200 × magnification.

than that of the steel substrate evaluated at 0.5 and close to ML1-Sa2 and ML2-Sa2 coatings COF values.

3.3. Damage analysis

Figs. 6–10 demonstrate the application of SEM/EDS-WDS analysis in the characterization of the worn films. The micrographs were taken on the worn surface of CrN and TiN/CrN coatings generated after 800 and 2000 cycles of unlubricated sliding against a 100Cr6 steel ball.

Fig. 6(a) shows the worn surface morphology of CrN1-Sa1 and CrN2-Sa2 coatings deposited on the Sa1 and Sa2 steel substrate, respectively. No significant wear topography difference is observed. Both samples manifested total delamination of the CrN coating and uniform oxide film

covered the worn surfaces as revealed by the EDS analysis in Fig. 6(b). This indicates that tribochemical oxidation occurred between the Fe atoms present in the exposed steel substrate and the O₂ atoms present in the atmosphere (see e.g., in Refs.[42,47]).

Fig. 7 gives SEM images of the ML1, the ML2 and the ML3 coatings. The tribofilm formed on the worn surfaces consist of nanoscale attachments generated from the coating breakage, fracture, and spalling wears; these were stacked onto the sliding contact zone. Effectively, during sliding friction, the contact formation, the adhesive attraction, shocks and interlock between asperities on the real contact area, generated elastic and plastic deformations under the applied load. The contact stress became predominant due to the higher frictional heat and frictional energy.[40,43] At this critical point, the film delamination

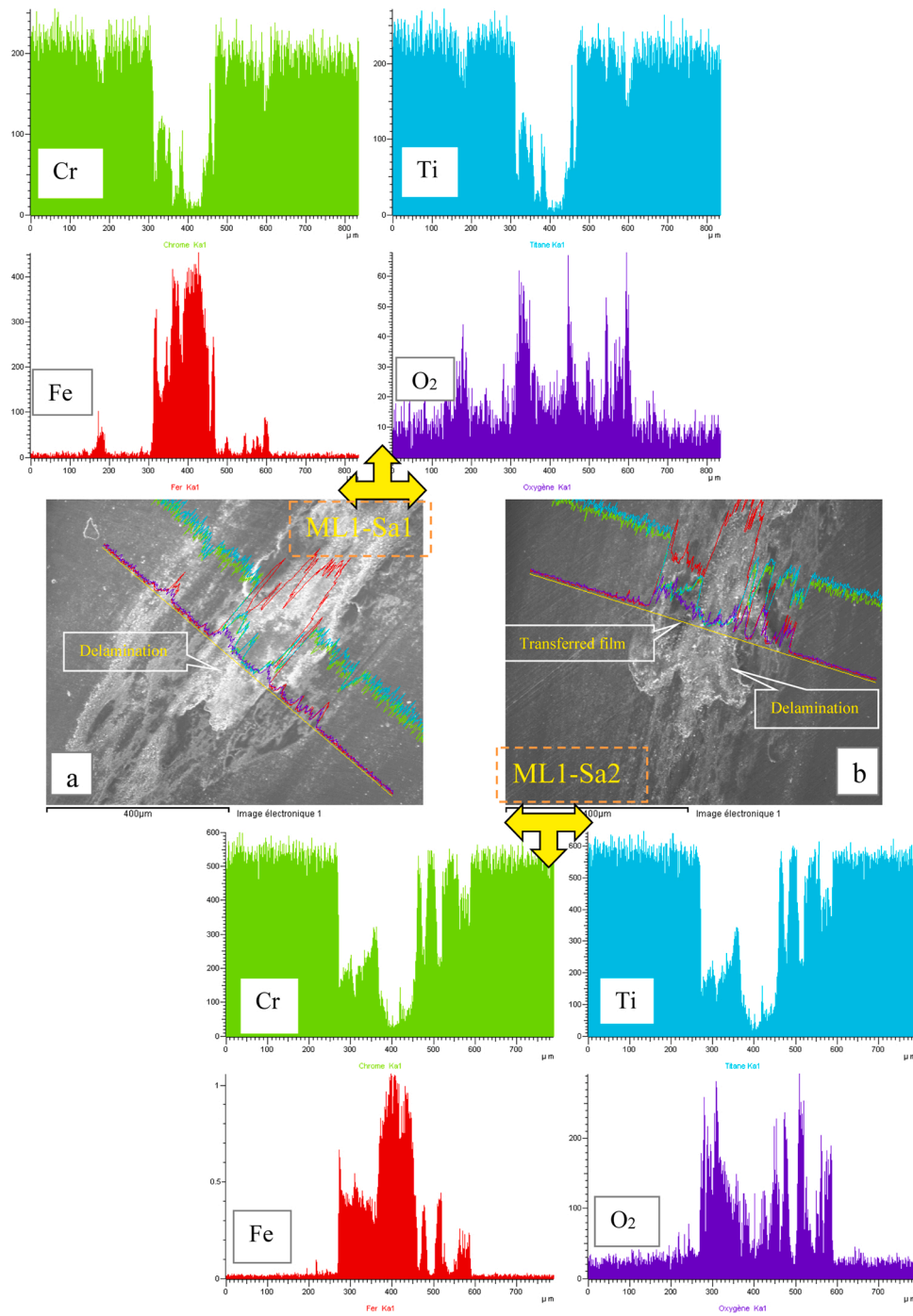


Fig. 8. Worn surface SEM-micrographs with their corresponding EDS profiles of the TiN/CrN multilayered coatings with $\Lambda = 20$ nm deposited on (a) Sa1 surface substrate and (b) Sa2 surface substrate.

took place. The debris were then subjected to further breaking, crushing, and oxidation. Ti, Cr (coating elements), Fe and O_2 chemical elements presence was confirmed by the EDS chemical analysis (Figs. 8, 9 and 10, of ML1, ML2 and ML3 coatings, respectively) carried out in the wear track, and also in the accumulated wear debris (Fig. 7. (a)) on the edges of the wear track. As a result, the generated wear debris were accumulated on the wear track resulting in a slight adhesion feature consistent with the oscillation of COF (according to the Bowden and al. approach [44]) as observed in the friction curves Fig. 4. The temperature generated from frictional heating, by the conversion of shearing strain energy, lead to chemical reactions activation.

The tribofilm present in the wear track of the ML1-Sa1 coating (Fig. 7

(a)) exhibited fish-scale like morphology (Fig. 7(i)). Such morphology suggested, adhesive flow of tribofilm have been driven by tangential load. Similar results have also been observed on other coatings [40]. On the other hand, the ML1-Sa2 worn surface (Fig. 7(b)) exhibited dark patches (Fig. 7 (ii)). These transferred layers were basically constituted of the transferred iron material adhering to delaminated substrates. The strapped coating exposed the substrate which resulted in steel-to-steel friction. Thus, element from the counterpart surface were transferred over the TiN/CrN multilayer surface under the effect of the high temperature generated by sliding and friction. The dry sliding, the contact stress, as well as the chemical reactivity provoke delamination, severe oxidative and adhesive wear as revealed in the EDS analysis (Fig. 8(a

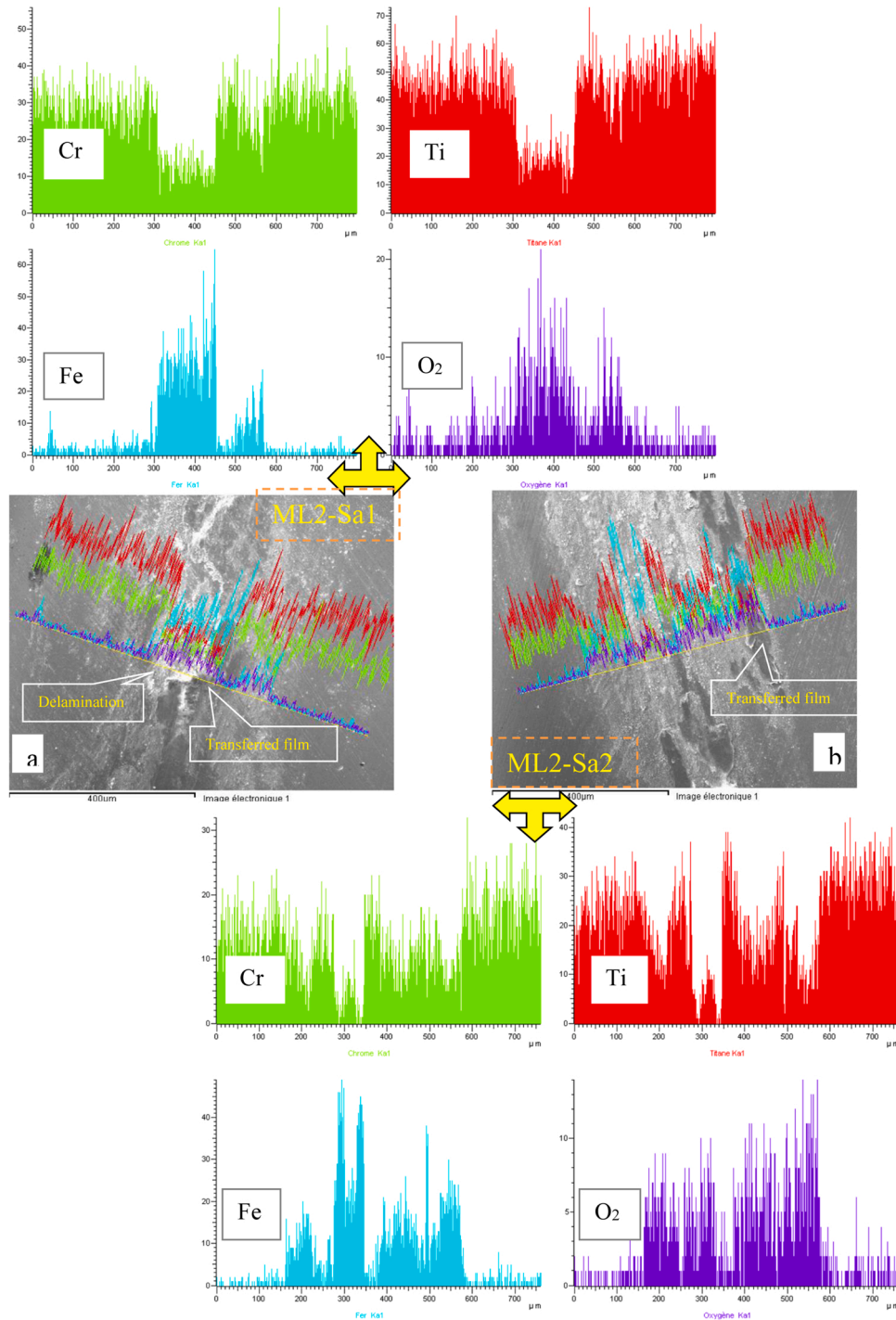


Fig. 9. Worn surface SEM-micrographs with their corresponding EDS profiles of the TiN/CrN multilayered coatings with $\Lambda = 12$ nm deposited on (a) Sa1 surface substrate and (b) Sa2 surface substrate.

and b)).

Regarding the ML2-(Sa1 and Sa2) coatings, almost no surface delamination has been observed (Fig. 7(c and d)). This is also shown by optical profilometry (Fig. 12 (a)). Nevertheless, some delamination was observed on the wear profiles of the ML2-Sa1 coating (Fig. 7(c) and 9 (a)) as compared with that deposited on rougher substrate (Figs. 7(d) and 9(b)). The SEM images of the ML1 and the ML2 coated rough substrates surfaces (Sa2), respectively provide evidence of better wear resistance with lower damage density. The ML1-Sa2 and the ML2-Sa2 higher hardness, as compared with those deposited on smoother substrate surface, withstood better wear despite their higher roughness. In

addition, the ML1-Sa2 coefficient of friction presented a more stable curve with no peak as illustrated in Fig. 4(b). Moreover, the coefficient of friction of the ML2-Sa2 coating showed a lower average value than that of ML2-Sa1 coating thus contributing to a better wear resistance.

Uniform oxide films covered the ML3-(Sa1 and Sa2) worn surfaces (Fig. 7(e and f)), indicating that tribochemical oxidation had occurred under atmospheric environment. Although the wear mechanisms observed on the three multilayers are similar, the ML3 coatings appear to have suffered to more severe wear (Fig. 10). Furthermore, contrary to the ML1 and ML2 coatings wear behavior, the ML3-Sa2 coating deposited on a rougher surface substrate (Fig. 10 (b)) showed lower wear

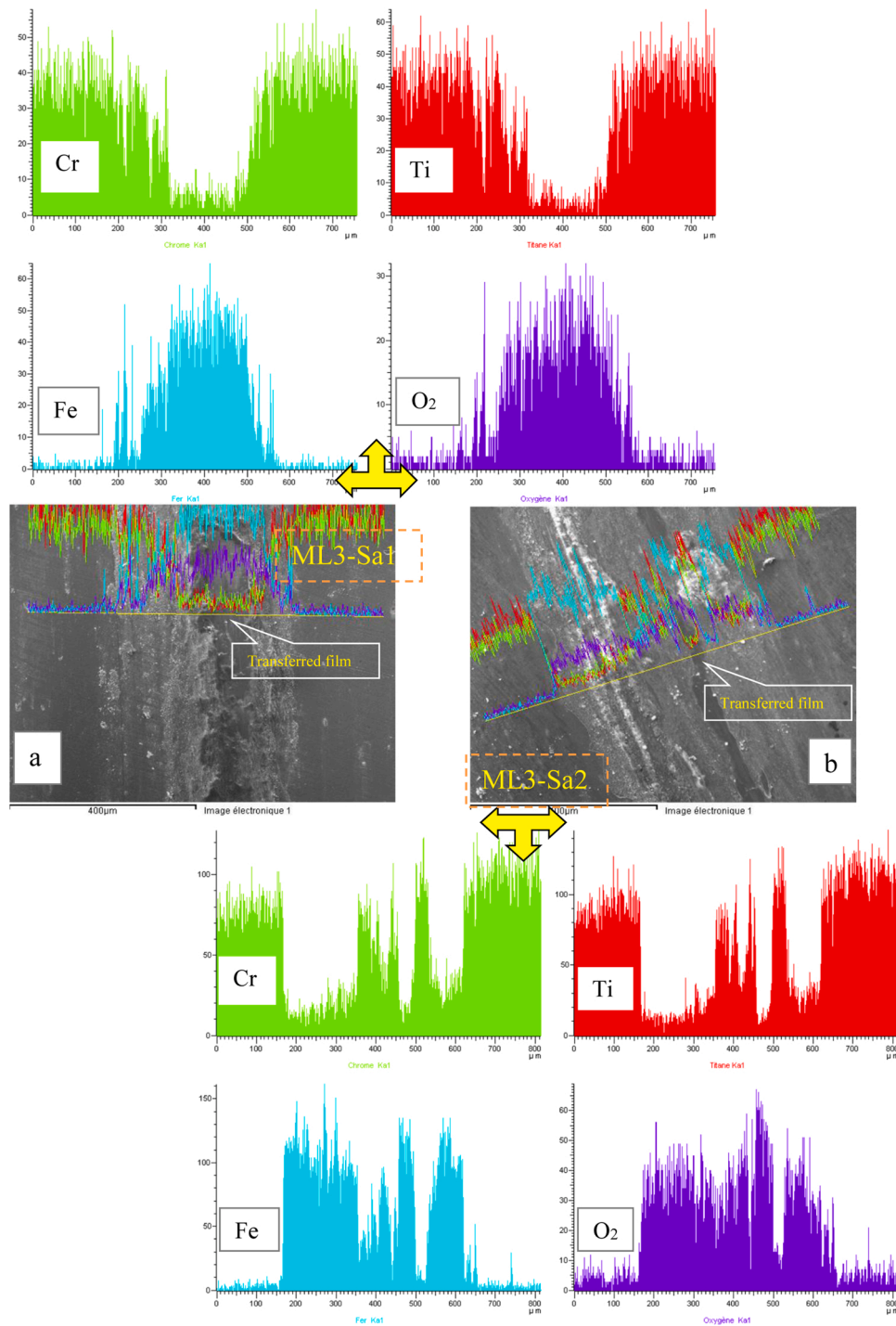


Fig. 10. Worn surface SEM-micrographs with their corresponding EDS profiles of the TiN/CrN multilayered coatings with varying $\Lambda = 40\text{--}10\text{ nm}$ deposited on (a) Sa1 surface substrate and (b) Sa2 surface substrate.

resistance than the ML3-Sa1 coating deposited on a smoother surface substrate (Fig. 10 (a)). Indeed, as compared to the ML2-Sa2 coating which still exhibited a major coating content (spectra 1 and 3) with some transferred films (spectrum 2) (EDS spectra in Fig. 11 (a)), the ML3-Sa2 coating was dominated by a severe oxidative wear (presence of Fe and O₂ in spectra 2 and 4) with a progressive disappearance of chromium and titanium, as shown in EDS spectra in Fig. 11 (b). Nevertheless, when the EDS software quantifies spectra, the calibration which is based on homogeneous interaction volumes, must be considered. It then applies very specific corrections to achieve the best precision. With these more or less worn and plasticized layers, of unknown thicknesses, the error

would be very significant, especially since an oxidation process takes place and it is not known which elements are more or less oxidized.

As illustrated by the optical analysis, the TiN/CrN multilayer with low period, deposited on the rough steel substrate surface, outperforms the other two coatings in terms of wear resistance (Fig. 12 (a)). A quantity of the counterpart mater was transferred on the wear track. Whilst, the TiN/CrN multilayer with varying periods is found to be less resistant, some coated delamination and transferred particles adherent to the worn surface were observed in Fig. 12 (b). However, all the TiN/CrN multilayers investigated were highly more wear resistant than the CrN monolayer which was dominated by abrasion groove formation and

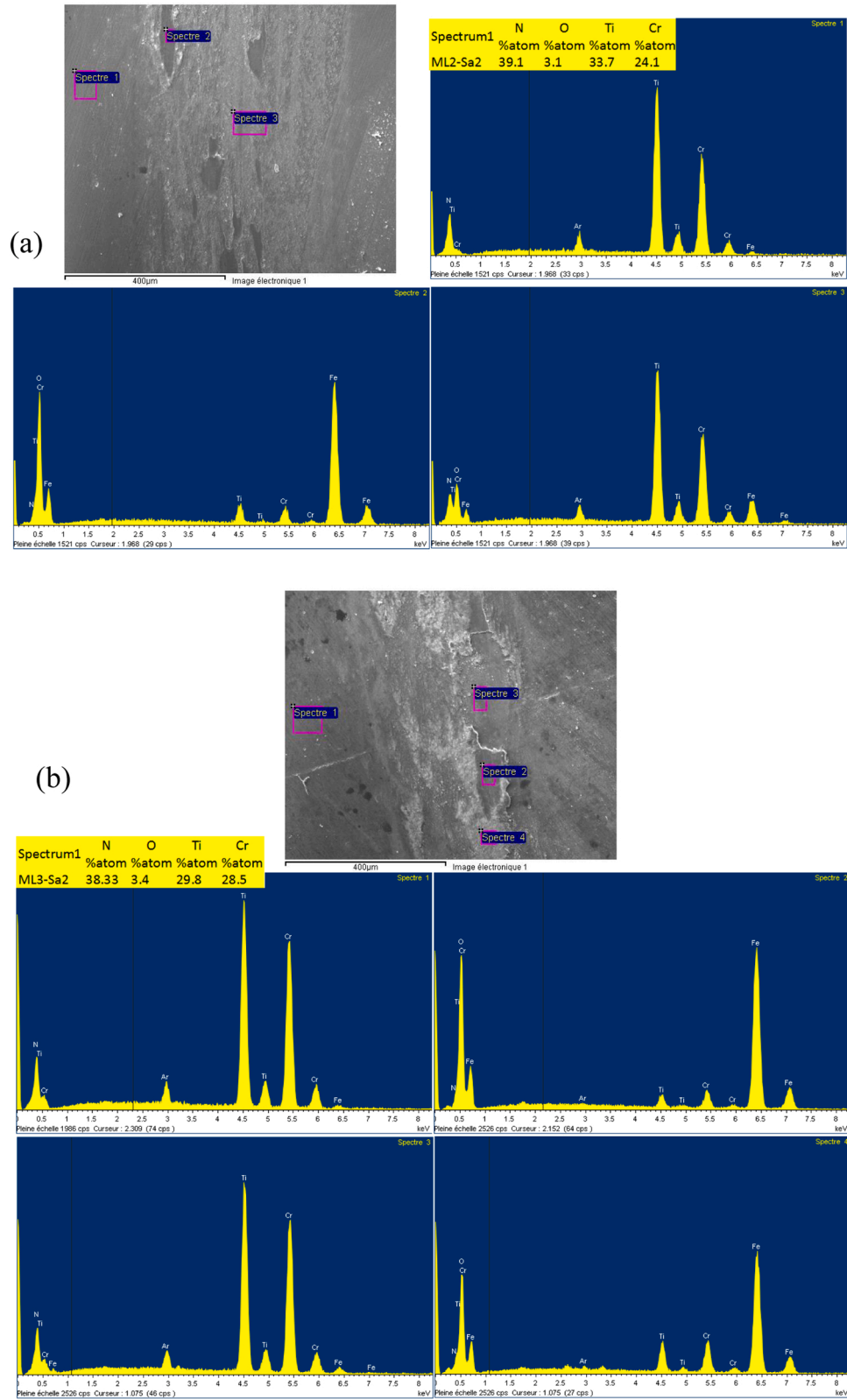


Fig. 11. EDS chemical analysis of the worn surface (a) ML2-Sa2 and (b) ML3-Sa2.

fatigue delamination wear mechanisms observed in the worn surface (Fig. 12(c)).

Although it was difficult to assess the coating wear rates, given that the damage was not uniform over the entire wear track (variable delamination distribution, size and intensity), the wear volume of

analyzed coatings was estimated from optical profiles (Fig. 13) and wear rate (K_v) calculation, which is defined by the Archard equation (Eq. (1)).

$$K_v = \frac{V}{L \cdot F_N} \cdot H$$

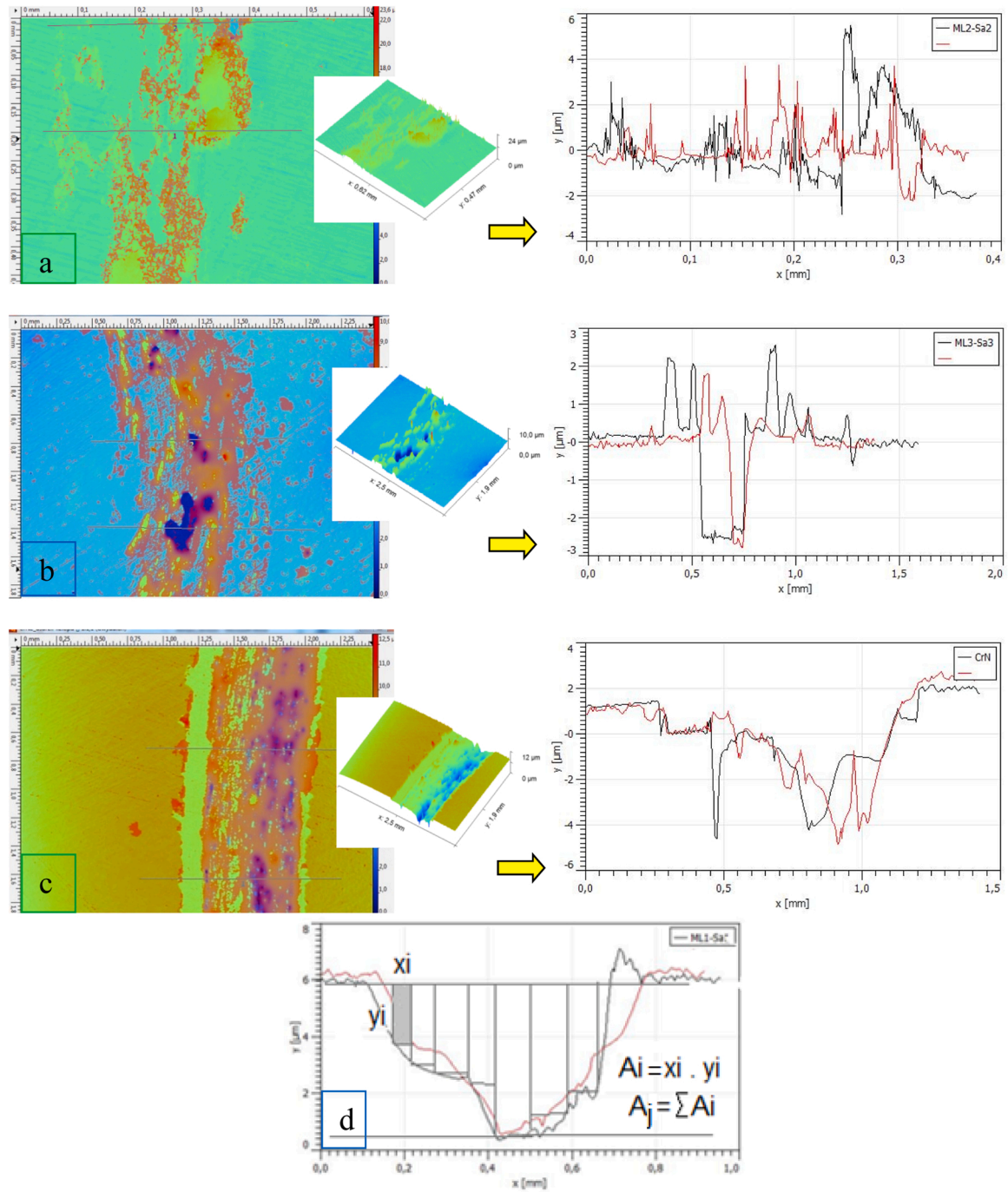


Fig. 12. Illustration of the in-situ wear depth profiles (2D and 3D) for:(a) ML2-Sa2, (b) ML3-Sa3, (c) CrN coatings and (d) the schematic illustration of the wear volume calculation.

with V the volume of wear, FN the normal load, L the sliding distance and H the hardness of the material tested.

To be able to obtain an estimate of the volume of wear, it was necessary to carry out careful examination of the wear tracks. Following the analysis of the entire wear track for each sample, it can be seen that the distribution of damage is random for each case and the depth and width are different across the wear track. It is therefore difficult to apply the commonly used method, based on calculating the wear volume from the following formula: $V = 2\pi \times r \times w \times d$ where r is the wear track radius, w the track width and d the track depth. The method of sections was used instead as it was found more suitable in our case.

The volume loss of the samples is determined by measuring the total

cross-sectional A_j from the elemental sections A_i , as illustrated in Fig. 12 (i), and using the following formula: $V = 2\pi \times r \times \frac{1}{n} \sum_0^n A_j$ where $2\pi \times r$ is the nominal circumference of the track and $\frac{1}{n} \sum_0^n A_j$ the average of a number n (depending on the state of the wear track) of measurements of the total cross-sectional area A_j (the transferred areas have been considered as well as the delaminated sections).

The use of this “unconventional” measurement technique (developed by Fliti R. [45]) has the sole aim of carrying out a comparative tribological evaluation between several samples subjected to the same experimental conditions. The results are shown in Table 1.

It can be noticed in Fig. 13 that the wear rates of the TiN/CrN multilayers with a constant Λ , deposited on rough steel substrate surface

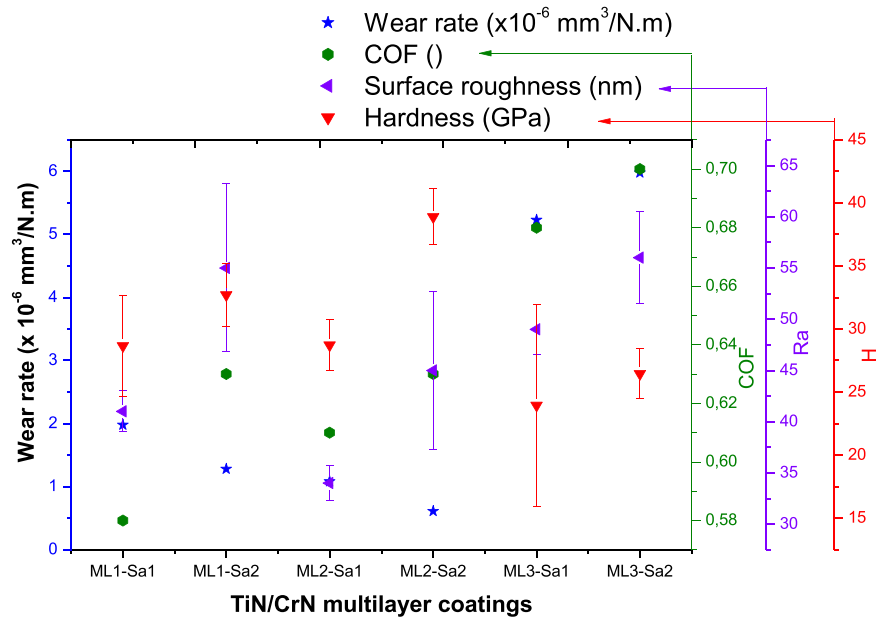


Fig. 13. Wear rate evolution with the coatings coefficient of friction, surface roughness and hardness.

Table 1
Wear rate of the TiN/CrN multilayer coatings.

	CrN	ML1		ML2		ML3	
		Sa1	Sa2	Sa1	Sa2	Sa1	Sa2
Wear Volume ($\times 10^{-3} \text{ mm}^3$)	96.13	0.783	0.577	0.215	0.120	1.475	2.182
Wear rate ($\times 10^{-6} \text{ mm}^3/\text{N.m}$)	640	5.22	3.85	1.43	0.802	9.83	14.55

are lower than ones of the same films deposited on the smooth steel substrate surface. In contrary, the TiN/CrN multilayers with a varying Λ , deposited on rough steel substrate surface (ML3-Sa2) showed the highest wear rate, estimated at $14.55 \times 10^{-6} \text{ mm}^3/\text{N.m}$. This is in agreement with results from the micrographic and optical analyze.

The greater the friction coefficient, the greater the wear rate, this has been reported by many authors [43,46,47] who have claimed that the Lining wear correlates well with friction performance. Indeed, this can be observed on ML3 coatings which showed the highest coefficients of friction. However, although the coefficients of friction of the ML1-Sa2 and ML2-Sa2 coatings are higher compared to the respective ML1-Sa1 and ML2-Sa1 coatings deposited on less rough substrate surfaces, it can still be noticed that their wear rates are lower. Indeed, the wear rate does not depend only on the coefficient of friction but high hardness and good adhesion are believed to be contributing factors as well. Nevertheless, the TiN/CrN multilayer coating exhibited approximately 100 times lower wear rate than the CrN monolayer coatings submitted to the same tribological test.

During sliding tests, adhesive wear mechanism initiated primarily by delamination generated by the fatigue action was combined with oxidative wear mechanism. The coating suffered chemical reactions generated from frictional heating and surface material transfer with formation of some non uniform oxide films on the worn surface [48]. On the other hand, the damage remains localized in some areas of the wear track. Dinesh Kumar et al. [35] confirm that the wear mechanism of TiN/CrN coating is dominated by oxidative and adhesive wears. Friction behavior of the film is related to various factors such as hardness, fracture toughness, stress and strain development during sliding contact of two different sliding bodies. It is largely affected by the crack nucleation and propagation [49,50], reactive and transfer layer formation [42] and wear particle formation [27].

Decreasing the bi-layer period from 20 nm to 12 nm lead to rough-

ness and wear rate decrease. On the other hand the COF remained relatively moderate. Further decreasing in bi-layer thickness by varying period ($\Lambda_3 = \sim 40\text{--}10 \text{ nm}$), lead to significant rise in tribological parameters, reaching maximum COF and wear rate values of 0.7 and $14.55 \times 10^{-6} \text{ mm}^3/\text{N.m}$, respectively. The tribological property improvements of the multilayer coating are in accordance with the mechanical analysis results in previous work. [33] The high resistance of the TiN/CrN coating with Λ_2 ($\sim 12 \text{ nm}$, ratio 1.7:1), compared to the other films, can be explained by its higher number of interfaces (300 interfaces) and its finer structure (crystallite size 6.9 and 11.5 nm, for ML2-Sa1 and ML2-Sa2, respectively). This resulted in ML2-Sa2 better resistance to deformation ($H^3/E^*^2 = 0.20 \text{ GPa}$) and better toughness ($L_{C1} = 4.3 \text{ N}$). Indeed, it has been reported that the multilayer better resistance to cracking is attributed to the stratified structure which would limit the propagation of cracks by decohesion of the successive layers at the interfaces and would thus increase the multilayer coating resistance (similar trend are reported in Refs.) [34,35,51]. Furthermore, owing to the lower individual layer thickness, the delaminated particle sizes released during friction are smaller and its wear rate is therefore lower than the other coatings. The coatings deposited on the rougher substrate (ML1-Sa2 and ML2-Sa2) showed particularly better wear resistance. Their higher hardness contributed to this improvement despite the fact that their coefficient of friction presents higher values than those of the coating deposited on the less rough substrate. The wear resistance improvement of the coatings prepared on rougher substrates is also attributed to the mechanical interlocking effect of the coating to the substrate asperities which acts on the adhesion of the layers [43], thus reinforcing their resistance to cracking and fracture.

4. Conclusion

The influence of bilayer period and substrate roughness on the wear

resistance of TiN/CrN multilayer coatings has been assessed. It was evaluated by wear testing carried out on different TiN/CrN multilayer coatings with constant and varying periods, elaborated by DC magnetron sputtering on steel substrates with two different surface roughnesses. The analysis of the obtained results allow to the following conclusions may be drawn:

- The TiN/CrN multilayer coatings with constant period have friction coefficients close to CrN monolayer coating and higher COF for the multilayer with varying period. The coatings suffered chemical reactions generated from friction heating and surface material transfer with formation of some non uniform oxide films on the sliding surface.
- Decreasing in bilayer thickness period of the TiN/CrN multilayer coatings improved their sliding wear resistance by enhancing their mechanical behavior. It has also lead to systematically increase the interface number by increasing the failure deflection and hence to decrease the detached particle size.
- Wear resistance enhancement of the coatings prepared on rougher substrate surfaces, despite the fact that their coefficient of friction presents higher value than those of the coating deposited on the smoother substrate surfaces, is attributed to the mechanical interlocking effect of the coating to the substrate asperities (by increasing the substrate area) which acts on the layer adhesion, thus reinforcing their resistance to cracking and fracture.

However, varying thickness period and also increasing the substrate surface roughness did not show any significant wear resistance improvement, as opposed to the constant period. Nonetheless, the multilayer coating wear resistance remains higher than the CrN monolayer. These results are correlated to previous TiN/CrN multilayer mechanical results. Further investigation into wear mechanisms in multilayers are yet required in order to better understand the tribomechanical behavior and how it is related to multilayer period thickness and surface roughness.

Declaration of Competing Interest

The authors declare that they have no known competing financial interests or personal relationships that could have appeared to influence the work reported in this paper.

Data availability

The authors do not have permission to share data.

Acknowledgements

A major part of this work was carried out at the LaBoMaP, Arts et Metiers Institute of Technology, Rue Porte de Paris Cluny 71250, France. The authors would especially like to thank Dr. Aurélien Besnard for his assistance in the production of coatings and Denis Lagadrillère for the SEM analysis.

References

- [1] Jiao Z, Peterkin S, Felix L, Liang R, Oliveira PJ, Schel N, Scotchmer N, Toyserkani E, Zhou Y. Surface modification of 304 stainless steel by electro-spark deposition. *JMEPEG* 2018;27(9):4799–809. <https://doi.org/10.1007/s11665-01863579-0>.
- [2] El Laithy M, Wang L, Harvey T, Schwedt A, Kruhoeffer Wolfram, Mayer Joachim. "Initiation and evolution of butterflies in rollerbearings due to rolling contact fatigue,". *Tribol Int* 2023. <https://doi.org/10.1016/j.triboint.2023.108987> (Pre-proof).
- [3] Masmoudi YA, Chaouche B, Mokhtari A. Effect of rectangular rough dimples of textured surface on tribological behavior of a hydrodynamic journal bearing. *Tribol Int* 2023;189:108945. <https://doi.org/10.1016/j.triboint.2023.108945>.
- [4] Zheng C, Liu Y, Chen C, Qin J, Ji R, Cai B. Numerical study of impact erosion of multiple solid particles,". *Appl Surf Sci* 2017;423:176–84. <https://doi.org/10.1016/j.apsusc.2017.06.132>.
- [5] Bonua Venkataramana, Jeevitha M, Praveen Kumar V, Bysakh Sandip, Barshilia Harish C. Ultra-thin multilayered erosion resistant Ti/TiN coatings with stress absorbing layers. *Appl Surf Sci* 2019;478:872–81. <https://doi.org/10.1016/j.apsusc.2019.02.012>.
- [6] Lopez-Urunuela F, Fernandez-Diaz B, Pagano F, Lopez-Ortega A, Pinedo B, Bayon R, Aguirrebeitia J. Broad review of "White Etching Crack" failure in wind turbine gearbox,". *In. J. of Fatigue* 2021;145:106091. <https://doi.org/10.1016/j.jfatigue.2020.106091>.
- [7] Ducros C, Benevent V, Sanchette F. Deposition, characterization and machining performance of multilayer PVD coatings on cemented carbide cutting tools,". *Surf Coat Technol* 2003;163-164:681–8. <https://doi.org/10.1016/j.triboint.2023.108945>.
- [8] Beliardouh NE, Bouzid K, Nouveau C, Tlili B, Walock MJ. Tribological and electrochemical performances of Cr/CrN and Cr/CrN/CrAlN multilayer coatings deposited by RF magnetron sputtering (Part B) *Tribol Int* 2015;82:443–52. <https://doi.org/10.1016/j.triboint.2014.03.018>.
- [9] Bouamerene MS, Nouveau C, Aknouché H, Zerizer A, Atmani TD, Challali M. "A Study of Cr/CrN and Cr/CrN/CrAlN Multilayer Coatings for Permanent Mold Castings of Aluminum Alloys: Wear and Soldering Tendency,". *J Mater Enginerring Struct* 2021;8:83–94. e-ISSN: 2170-127X.
- [10] Gallegos-Cantú S, Hernandez-Rodriguez MAL, Garcia-Sanchez E, Juarez-Hernandez A, Hernandez-Sandoval J, Cue-Sampedro R. Tribological study of TiN monolayer and TiN/CrN (multilayer and superlattice) on Co–Cr alloy. *Wear* 2015;330-331:439–47. <https://doi.org/10.1016/j.wear.2015.02.010>.
- [11] Ramoul CE, Nouveau C, Beliardouh NE, Kaleli EH, Ourdjini A, Ghelloudj O, Demirta S, Gharbi A, Bouzid K. "Mechanical properties and bio-tribological performance of PVD (Ta/ZrN)n multilayer coatings on UHMWPE in bovine serum lubrication,". *Int Journal Adv Manuf Technol JAMT* 2022;121:7527–38. <https://doi.org/10.1007/s00170-22-09854-1>.
- [12] Martínez-Cruz FS, Vite-Torres M, Moran-Reyes A. Wear and friction characterisation of some restorative dental materials. *Tribol Mater* 2022;1(1):27–34. <https://doi.org/10.46793/tribomat.2022.004>.
- [13] Mayrhofer PH, Geir M, Locker C, Chen L. Influence of deposition conditions on texture development and mechanical properties of TiN coatings. " *Int J Mater Res* 2009;100(8):1052–8. <https://doi.org/10.3139/146.110159>.
- [14] Vera EE, Vite M, Lewis R, Galardo EA, Laguna-Camacho JR. A study of the wear performance of TiN, CrN and WC/C coatings on different steel. *Wear* 2011;271:2116–24. <https://doi.org/10.1016/j.wear.2010.12.061>.
- [15] Zhang Xin, Tian Xiu-Bo, Zhao Zhi-Wei, Gao Jian-Bo, Zhou Yan-Wen, Gao Peng, Guo Yuan-Yuan, Lv Zhe. Evaluation of the adhesion and failure mechanism of the hard CrN coatings on different substrates. *Surf Coat Technol* 2019;364:135–43. <https://doi.org/10.1016/j.surfcoat.2019.01.059>.
- [16] Zeng XT, Zhang S, Sun CQ, Liu YC. "Nanometric-layered CrN/TiN thin films: mechanical strength and thermal stability,". *Thin Solid Films*, C 2003;424:99–102. [https://doi.org/10.1016/S0040-6090\(02\)00921](https://doi.org/10.1016/S0040-6090(02)00921).
- [17] Lomello F, Yazdi MArab Pour, Sanchette F, Schuster F, Tabarant M, Billard A. Temperature dependence of the residual stresses and mechanical properties in TiN/CrN nanolayered coatings processed by cathodic arc deposition. *Surf Coat Technol* 2014;238:216–22. <https://doi.org/10.1016/j.surfcoat.2013.10.079>.
- [18] Danie R, Meindlhume M, Zalesak J, Sartory B, Zeilinger A, Mitterer C, et al. Fracture toughness enhancement of brittle nanostructured materials by spatial heterogeneity: A micromechanical proof for CrN/Cr and TiN/SiOx multilayers. *Mater Des* 2016;104:227–34. <https://doi.org/10.1016/j.matdes.2016.05.029>.
- [19] Barshilia Harish C. Surface Modification Technologies for Aerospace and Engineering. *Trans Indian Natl Acad Eng* 2021;6:173–88. <https://doi.org/10.1007/s41403-021-00208-z>.
- [20] Su CY, Pan CT, Liou TP, Chen PT, Lin KT. Investigation of the microstructure and characterizations of TiN/CrN nano-multilayer deposited by unbalanced magnetron sputter process. *Surf Coat Technol* 2008;203:657–60. <https://doi.org/10.1016/j.surfcoat.2008.05.057>.
- [21] Khadem M, Penkov OV, Yang H-K, Kim D-E. Tribology of multilayer coatings for wear reduction: A review. *Friction* 2017;5(3):248–62. <https://doi.org/10.1007/s40544-017-0181-7>.
- [22] Falsafein M, Ashrafizadeh F, Kheirandish A. "Influence of thickness on adhesion of nano-structured multilayer CrN/CrAlN coatings to stainless steel substrate,". *Surf Interfaces* 2018;13:178–85. <https://doi.org/10.1007/s11771-018-3755>.
- [23] Paulitsch J, Maringer C, Mayrhofer PH. Low Friction CrNMPP/TiNDCMS Multilayer Coatings. *Tribol Lett* 2012;46:57–93. <https://doi.org/10.1007/s11249-012-9922-y>.
- [24] Mutyala Kalyan C, Ghanbari E, Doll GL. Effect of deposition method on tribological performance and corrosion resistance characteristics of CrxN coatings deposited by physical vapor deposition. *Thin Solid Films* 2017;636:232–9. <https://doi.org/10.1016/j.tsf.2017.06.013>.
- [25] Aissani L, Alhussein A, Ayad A, Nouveau C, Zgheib E, Belgroune A, Zaabat M, Barille R. Relationship between structure, surface topography and tribomechanical behavior of Ti-N thin films elaborated at different N2 flow rates. *Thin Solid Films* 2021;724:138598. <https://doi.org/10.1016/j.tsf.2021.138598>.
- [26] Xie Qi, Fu Zhiqiang, Liu Ziyi, Yue Wen, Kang Jiajie, Zhu Lina, Wang Chengbiao, Lin Songsheng. "Improvement of microstructural and tribological properties of titanium nitride by optimization of substrate bias current,". *Thin Solid Films* 2022;749:139181. <https://doi.org/10.1016/j.tsf.2022.139181>.
- [27] Jean Denape. "Third body concept and hard particle behavior in dry friction sliding conditions,". *Tribol Asp Mod Aircr Ind, Trans Tech Publ* 2014:1–12. <https://doi.org/10.4028/www.scientific.net/KEM.0.1>.

- [28] Takadoun J, Houmid Bennani H. "Influence of substrate roughness and coating thickness on adhesion, friction and wear of TiN films,". *Surf. Coat. Technol*, 96; 1997. p. 272–82. [https://doi.org/10.1016/S0257-8972\(97\)00182-5](https://doi.org/10.1016/S0257-8972(97)00182-5).
- [29] Kammingaa J-D, van Essen P, Hoy R, Janssen GCAM. Substrate dependence of the scratch resistance of CrN_x coatings on steel. *Tribol Lett* 2005;19(2):65–72. <https://doi.org/10.1007/s11249-005-5081-8>.
- [30] Xian Guang, Xiong Ji, Fan Hongyuan, Jiang Fan, Guo Zhixing, Zhao Haibo, Xian Lijun, Jing Zhengbiao, Liao Jun, Liu Yi. Investigations on microstructure, mechanical and tribological properties of TiN coatings deposited on three different tool materials. *Int J Refract Met Hard Mater* 2022;102:105700. <https://doi.org/10.1016/j.ijrmhm.2021.105700>.
- [31] Liu Z-J, Shum PW, Shen YG. Surface growth of (Ti,Al)N thin films on smooth and rough substrates. *Thin Solid Films* 2006;496:326–32. <https://doi.org/10.1016/j.tsf.2005.08.380>.
- [32] Dinesh Kumar D, Kumar N, Kalaiselvam S, Dash S, Jayavel R. Substrate effect on wear resistant transition metal nitride hard coatings: Microstructure and tribo-mechanical properties. *Ceram Int* 2015;41:9849–61. <https://doi.org/10.1016/j.ceramint.2015.04.059>.
- [33] Atmani TD, Gaceb M, Aknouche H, Nouveau C, Bouamrene MS. "Parametric study of mechanical properties of nanocrystalline TiN/CrN multilayer coatings with a special focus on the effect of coating thickness and substrate roughness. *Surf Interfaces* 2021;23:101001. <https://doi.org/10.1016/j.surf.2021.101001>.
- [34] Barshilia HC, Rajam KS. Deposition of TiN/CrN hard superlattices by reactive d.c. magnetron sputtering,". *Bull Mater Sci* 2003;26(2):233–7. <https://doi.org/10.1007/BF02707797>.
- [35] Dinesh Kumar D, Kumar N, Kalaiselvam S, Thangapan R, Jayael R. "Film thickness effect and substrate dependent tribo-mechanical,". *Surf Interfaces* 2018;12:78–85. <https://doi.org/10.1016/j.surf.2018.05.002>.
- [36] Murwamadala RD, Rao VV. Wear performance of AISI 4140 low-alloy steel PVD coated with TiN. *Adv Mater Process Technol* 2023. <https://doi.org/10.1080/2374068X.2023.2185439>.
- [37] Fernández-Valdés D, Meneses-Amador A, López-Liévano A, Ocampo-Ramírez A. "Sliding wear analysis in borided AISI 316L steels,". *Mater Lett* 2021;285:129138. <https://doi.org/10.1016/j.matlet.2020.129138>.
- [38] Wu PQ, Drees D, Stals L, Celis JP. Comparison of wear and corrosion wear of TiN coatings under uni- and bidirectional sliding. *Surf Coat Technol* 1999;113:251–8. [https://doi.org/10.1016/S0257-8972\(99\)00007-9](https://doi.org/10.1016/S0257-8972(99)00007-9).
- [39] Zhou YM, Asaki R, Higashi K, Soe WH, Yamamoto R. Sliding wear behavior of polycrystalline TiN/CrN multilayers against an alumina ball. *Surf Coat Technol* 2000;130:9–14. [https://doi.org/10.1016/S0257-8972\(00\)00674-5](https://doi.org/10.1016/S0257-8972(00)00674-5).
- [40] Luo Q. Electron microscopy and electroscopy in the analysis of friction and wear mechanisms. *Lubricants* 2018;6:58. <https://doi.org/10.3390/lubricants6030058>.
- [41] Chen L, Zhang Z, Lou M, Xu K, Wang L, Meng F, Music D. High-temperature wear mechanisms of TiNbWN films: Role of nanocrystalline oxides formation. *Friction* 2023;11(3):460–72. <https://doi.org/10.1007/s40544-022-0621-x>.
- [42] Luo Q. Origin of friction in running-in sliding wear of nitride coatings. *Tribol Lett* 2010;37:529–39. <https://doi.org/10.1007/s11249-009-9548-x>.
- [43] Kumar DDinesh, Kumar N, Kalaiselvam S, Dash S, Jayavel R. Wear resistant super-hard multilayer transition metal-nitride coatings. *Surf Interfaces*, " *Surf Interfaces* 2017;7:74–82. <https://doi.org/10.1016/j.surf.2017.03.001>.
- [44] Bowden FP, Tabor D. *The Friction and Lubrication of Solids, Part I*. Oxford: Clarendon Press; 1950.
- [45] Fliti Romain, Caractérisation en usure de revêtements par tribométrie haute température pour les applications mécaniques, MSc report, 2012, ENSAM of Cluny.
- [46] Zhou YM, Azaki R, Soe WH, Yamamoto R, Chen R. Hardness anomaly, plastic deformation work and fretting wear properties of polycrystalline TiN/CrN multilayers. *Wear* 1999;236:159–64. [https://doi.org/10.1016/S0043-1648\(99\)00272-0](https://doi.org/10.1016/S0043-1648(99)00272-0).
- [47] Ou YX, Lin J, Che HI, Sproul WD, Lei MK. Mechanical and tribological properties of CrN/TiN superlattice coatings deposited by a combination of arc free deep oscillation magnetron sputtering with pulsed dc magnetron sputtering. *Thin Solid Films* 2015;594:147–55. <https://doi.org/10.1016/j.tsf.2015.09.067>.
- [48] Zhou Fei, Suh Chang-Min, Kim Seock-Sam, Murakami Richi. "Sliding-wear behavior of TiN- and CrN-coated 2024 aluminum alloy against an Al₂O₃ ball,". *Tribol Lett* 2002;13(3):173–8. <https://doi.org/10.1023/A:1020103908345>.
- [49] Mendibide C, Fontaine J, Steyer P, Esnouf C. Dry sliding wear model of nanometer scale multilayered TiN/CrN PVD hard coatings. *Tribology Lett* 2004;17(4):779–89. <https://doi.org/10.1007/s11249-004-8086-9>.
- [50] Roa JJ, Rodríguez R, Lamelas V, Martínez R, Jiménez-Piqué E, Llanes L. Small scale fracture behaviour of multilayer TiN/CrN systems: Assessment of bilayer thickness effects by means of ex-situ tests on FIB-milled micro-cantilevers. *Surf Coat Technol* 2016;308:414–7. <https://doi.org/10.1016/j.surfcoat.2016.06.093>.
- [51] Mendibide C, Steyer P, Fontaine J, Goudeau P. Improvement of the tribological behavior of PVD nanostratified TiN/CrN coatings –An explanation. *Surf Coat Technol* 2006;201:4119–24. <https://doi.org/10.1016/j.surfcoat.2006.08.013>.